

Received November 16, 2019, accepted December 3, 2019, date of publication December 10, 2019, date of current version December 23, 2019.

Digital Object Identifier 10.1109/ACCESS.2019.2958645

Topology Optimization With Selective Problem Setups

JUNYU FU¹, JIAQI HUANG^{2,3}, AND JIKAI LIU^{2,3}

¹College of Mechanical and Vehicle Engineering, Taiyuan University of Technology, Taiyuan 030024, China

²Key Laboratory of High Efficiency and Clean Mechanical Manufacture, Ministry of Education, Center for Advanced Jet Engineering Technologies (CaJET), School of Mechanical Engineering, Shandong University, Jinan 250061, China

³Key National Demonstration Center for Experimental Mechanical Engineering Education, Shandong University, Jinan 250061, China

Corresponding author: Jikai Liu (jikai_liu@sdu.edu.cn)

This work was supported by the Key Laboratory of High-Efficiency and Clean Mechanical Manufacture, Ministry of Education, Shandong University.

ABSTRACT Topology optimization has demonstrated its power in structural design under a variety of physical disciplines. Generally, a topology optimization problem is formulated with clearly-defined problem setup. Both design domain shape and boundary condition are clearly-defined during pre-processing. Optimization with multiple choices of design domains or boundary conditions have to be performed with multiple runs of the algorithm to make the best choice among the selective problem setups. The computational cost is proportional to the number of problem setup choices which can be inefficient if a large number of choices are involved. Therefore, to save the computational cost, a novel topology optimization method is developed to solve the design problem with selective problem setups. This method employs a novel meshing strategy and material interpolation model to unify the multiple problem setups into a single optimization problem. Therefore, the optimization algorithm only runs once to concurrently derive the optimal structural shape and the best problem setup choice in a very efficient manner. In addition, the problem formulation is simple. Only $N + 1$ more design variables are added to realize the interpolation among $N + 1$ problem setup choices, other than the density variables for structural topology description. A few numerical examples will be demonstrated to show the effectiveness of the proposed method.

INDEX TERMS Additive manufacturing, selective design domains, selective boundary conditions, topology optimization.

I. INTRODUCTION

Topology optimization has been actively investigated since 1988 [1]. The homogenization method [1], SIMP (Solid Isotropic Material with Penalization) method [2], level set method [3], [4], ESO (Evolutionary Structural Optimization) method [5], MMC (Moving Morphable Components) method [6], and many others, have been developed, while the effectiveness of these methods in solving multidisciplinary structural optimization problems have been witnessed through a large amount of publications, as summarized in [7]–[10]. Among the many topics [11]–[14], design with geometric uncertainty is a special topic to address since manufacturing errors may severely deviate the as-fabricated solution from the ideal design. Sigmund and

his colleagues [15]–[17] developed the robust formulation to address the topology optimization formulation with manufacturing errors, wherein multiple realizations of the structure were derived through the erode and dilate filters. Methods were also developed with level set method by integrating stochastic perturbations to the level set-based geometry representation [18], [19]. Other than design with geometric uncertainty, topology optimization with uncertain/selective problem setups is also important but has been rarely focused. Here, the problem setup condition includes the design domain size and the boundary condition, while the uncertain/selective problem setups indicate the availability of multiple choices of different design domain sizes and/or boundary conditions. To better explain, Figure 1 demonstrates four similar but different problem setups, wherein both the design domain size and the loading position can be different among the setups. Note that, the symbols and the meshes in Figure 1 will be

The associate editor coordinating the review of this manuscript and approving it for publication was Chi-Tsung Cheng.

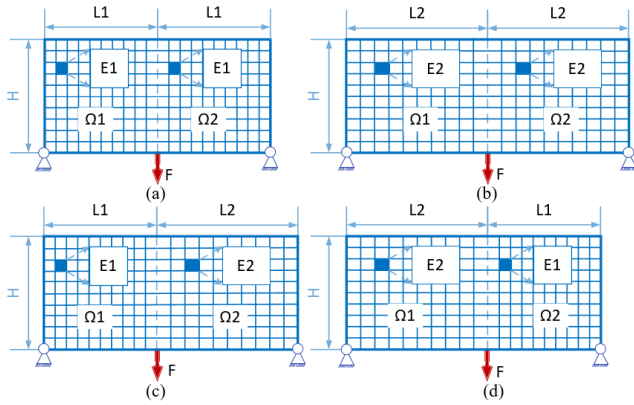


FIGURE 1. Different problem setups and the proposed meshing strategy.

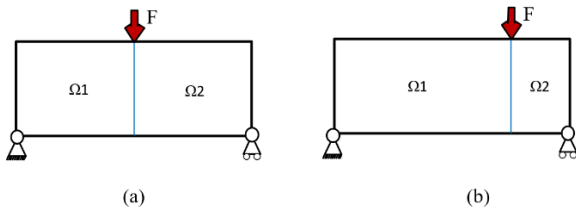


FIGURE 2. Setups of the MBB-beam problem: (a) sub-domain Ω_1 and Ω_2 both have the size of 40×40 ; (b) sub-domain Ω_1 has the size of 60×40 , and Ω_2 has the size of 20×40 .

explained in Section II when explaining the algorithm details. If the problem setups in Figure 1 are candidates to select, the design problem has to determine which setup could derive the best-performing structural topological design under the same amount of material consumption. A general idea is to perform the optimization multiple times and then, make the choice based on the optimized structural performances. However, multiple runs of the algorithm consume long computational time which is inefficient. Even if configured into a single topology optimization problem for multi-domain problems, multiple runs of finite element analysis have to be performed in each iteration, which does not obviously change the overall computational cost [20], [21]. Therefore, a novel topology optimization method is developed to solve the design problem with selective problem setups. This method employs a novel meshing strategy and material interpolation model to unify the multiple problem setups into a single optimization problem. Therefore, the optimization algorithm only runs once to concurrently derive the optimal structural shape and the best problem setup choice in a very efficient manner. Details of the proposed method will be specified in the next section.

Other than the theoretical novelty, the proposed method can be innovatively applied to design-for-additive manufacturing. In the past, quite some efforts have been spent on simplifying the topological designs to guarantee the manufacturability with traditional subtractive machining technology [22], [23]. However, emerging of the additive manufacturing technology enhances the capability of fabricating complex engineering structures, which greatly unleashes the power of topology optimization. Therefore, topology optimization for

additive manufacturing has been highly focused [24]. A typical example is that numerous multi-scale and multi-material topological structures have been designed and fabricated with additive manufacturing [25]–[37]. At the same time, new problems arise for design-for-additive manufacturing. As widely known, additive manufacturing is still not a fully developed technology [38], since many different processes and 3D printing machines exist and the derived mechanical properties of the same material from different processes and printing machines may vary significantly [39]. In addition, the 3D printers provide different chamber volumes. Therefore, design-for-additive manufacturing with multiple available 3D printers can be challenging, since the problem setup of topology optimization would be machine specific given the different material properties and design domain sizes. Therefore, the proposed topology optimization method with selective problem setups is just suitable to solve this challenging problem.

II. PROBLEM FORMULATION

A. SIMP METHOD

The SIMP (Solid Isotropic Material with Penalization) concept was proposed by Bendsøe [40], while the SIMP notion was raised by Rozvany *et al.* [41] in 1992. Numerous practical engineering problems have been solved with the SIMP method, wherein the objective function can be flexibly formulated to represent the structural compliance, stress, natural frequency, displacement, and many others. To make it simple, the compliance minimization problem is formulated below:

$$\begin{aligned} \min C(\boldsymbol{\rho}) &= \mathbf{U}^T \mathbf{F} = \mathbf{U}^T \mathbf{K} \mathbf{U} = \sum_{e=1}^N (\rho_e)^p \mathbf{u}_e^T \mathbf{k}_e \mathbf{u}_e \\ \text{s.t. } \frac{V(\boldsymbol{\rho})}{V_0} &= V_{\text{frac}} \\ \mathbf{K} \mathbf{U} &= \mathbf{F} \\ 0 < \rho_{\min} &\leq \rho_e \leq 1 \end{aligned} \quad (1)$$

where C is the structural compliance function, \mathbf{U} denotes the global displacement vector, \mathbf{K} is the global stiffness matrix, and \mathbf{F} is the global load vector. The elementwise density ρ_e will be optimized: 0 represents void and 1 for solid. The penalty p (usually ≥ 3) is employed to penalize the intermediate densities, so that to derive the black and white solution of the final design. ρ_{\min} is a small positive number to avoid the singularity problem in numerical calculation. $V(\boldsymbol{\rho})$ represents the volume of solids, where $V(\boldsymbol{\rho}) = \sum_{e=1}^N \rho_e V_{\text{element}}$. V_0 means the design domain volume. V_{frac} is the designated material volume fraction.

Sensitivity of the total compliance with respect to the pseudo-density is shown in (2). Details of the derivation is omitted and interested readers can refer to [2].

$$\frac{\partial C}{\partial \rho_e} = - \sum_{e=1}^N p (\rho_e)^{p-1} \mathbf{u}_e^T \mathbf{k}_e \mathbf{u}_e \quad (2)$$

To avoid the ‘‘checkerboard’’ issue [42], [43], sensitivity filter is employed through a convolution operation of

the original sensitivities. The modified sensitivity result is illustrated below:

$$\frac{\partial \widehat{C}}{\partial \rho_e} = \frac{1}{\rho_e \sum_{f=1}^N \widehat{H}_f} \sum_{f=1}^N \widehat{H}_f \rho_f \frac{\partial C}{\partial \rho_f} \quad (3)$$

where,

$$\widehat{H}_f = r_{\min} \text{dist}(e, f), \quad \{f \in N \mid \text{dist}(e, f) \leq r_{\min}\}, \quad e = 1, \dots, N \quad (4)$$

and $\text{dist}(e, f)$ denotes the distance between element e and f .

Optimality Criteria (OC) [44] method is employed as the optimizer to update the design variables. The main equations are illustrated in (5). $\eta = 0.5$ and m is the step limit. λ is the Lagrange multiplier.

$$x_{\text{new}} = \begin{cases} \max(x_{\min}, x_e - m) & \text{if } x_e B_e^\eta \leq \max(x_{\min}, x_e - m) \\ x_e B_e^\eta & \text{if } \max(x_{\min}, x_e - m) \leq x_e B_e^\eta \leq \min(1, x_e + m) \\ \min(1, x_e + m) & \text{if } \min(1, x_e + m) \leq x_e B_e^\eta \end{cases} \quad (5)$$

$$B_e = \frac{-\frac{\partial C}{\partial \rho_e}}{\lambda \frac{\partial V}{\partial \rho_e}}$$

B. THE MODIFIED METHOD

Before getting into the details of the proposed method, let's revisit the material interpolation model of multi-material problems. If design with two material options, equation (6) will be employed: ρ_2 realizes the interpolation between the different material types and ρ_1 interpolates between solid and void.

$$\mathbf{k}(\rho_1, \rho_2) = \rho_1^p (\rho_2^p \mathbf{k}^1 + (1 - \rho_2^p) \mathbf{k}^2) \quad (6)$$

where \mathbf{k}^1 is the element stiffness tensor with material type 1, and \mathbf{k}^2 is the element stiffness tensor with material type 2.

Then, the idea of multi-material interpolation can be inherited to address the topology optimization problem with selective problem setups. Specifically, different design domain sizes and loading positions will be provided by the different problem setups. The meshing strategy, as indicated by Figure 1, is proposed to address the distinctions among the problem setups. The key idea is to (i) discretize the different design domains with the same mesh scale, i.e. the same number of elements for each row or column; and (ii) the loading points should have the same nodal index in the finite element models. To fulfill these two requirements, the different candidate design domains are divided into two sub-domains $\Omega 1$ (left to the loading point) and $\Omega 2$ (right to the loading point), and each sub-domain, regardless of the size, is discretized with 10 by 10 uniform quadrilateral elements. Elements with different sizes and aspect ratios will be adopted to realize the meshing, for example the E1 of size L1/10 by H/10 and E2 of size L2/10 by H/10 in Figure. 1, which therefore, lead to two different element stiffness matrices: the $\bar{\mathbf{k}}^1$ and $\bar{\mathbf{k}}^2$, respectively. Then, regardless of the original

design domain sizes, we can think in the way that $\bar{\mathbf{k}}^1$ and $\bar{\mathbf{k}}^2$ are resulted by different materials instead of different element sizes. Therefore, the topology optimization problem with multiple selective problem setups has been transformed into an equivalent 'multi-material' topology optimization problem that can be completed with a single run of the algorithm. Finally, the new material interpolation model as illustrated in (7) is derived.

$$\mathbf{k}(\rho, y) = \rho^p (y^q \bar{\mathbf{k}}^i + (1 - y)^q \bar{\mathbf{k}}^j) \quad (7)$$

Note that, ρ is element-wisely different for the element pseud density representation; y is the design variable distinguishing two problem setups. The i and j may or may not be the same, depending on the meshes of the different problem setups.

Referring to the new interpolation model, the optimization problem with two selective problem setups is formulated in (8).

$$\begin{aligned} \min C(\rho) &= \mathbf{U}^T \mathbf{K} \mathbf{U} \\ &= \sum_{e=1}^N (\rho_e)^p \mathbf{u}_e^T (y^q \bar{\mathbf{k}}^i + (1 - y)^q \bar{\mathbf{k}}^j) \mathbf{u}_e \\ \text{s.t. } \frac{V(\rho, y)}{V_0} &= V_{\text{frac}} \\ V(\rho, y) &= \sum_{e=1}^N \rho_e [y V_{\text{element}}^i + (1 - y) V_{\text{element}}^j] \\ \mathbf{K} \mathbf{U} &= \mathbf{F} \\ 0 < \rho_{\min} &\leq \rho_e \leq 1 \\ 0 < y_{\min} &\leq y \leq 1 \end{aligned} \quad (8)$$

where ρ_e and y are the design parameters, $\rho_e \in [0, 1]$ is the element-wise material density, and a switch of y realizes the transition between two different problem setups. A different penalty parameter q is employed for design variable y , and its value will be discussed in the numerical implementation section.

Sensitivities of the objective function on ρ_e and y are demonstrated in (9) and (10), respectively.

$$\frac{\partial C}{\partial \rho_e} = -p (\rho_e)^{p-1} \mathbf{u}_e^T (y^q \bar{\mathbf{k}}^i + (1 - y)^q \bar{\mathbf{k}}^j) \mathbf{u}_e \quad (9)$$

$$\frac{\partial C}{\partial y} = - \sum_{e=1}^N (\rho_e)^p \mathbf{u}_e^T (q y^{q-1} \bar{\mathbf{k}}^i - q (1 - y)^{q-1} \bar{\mathbf{k}}^j) \mathbf{u}_e \quad (10)$$

The sensitivities of the volume fraction constraint can be similarly derived as shown below:

$$\frac{\partial V}{\partial \rho_e} = y V_{\text{element}}^i + (1 - y) V_{\text{element}}^j \quad (11)$$

$$\frac{\partial V}{\partial y} = \sum_{e=1}^N \rho_e (V_{\text{element}}^i - V_{\text{element}}^j) \quad (12)$$

A special discussion will be made here about the design update. The sensitivities on the element density ρ_e and the design variable y are calculated in an elementwise manner and in the domain integral form, respectively. Therefore,

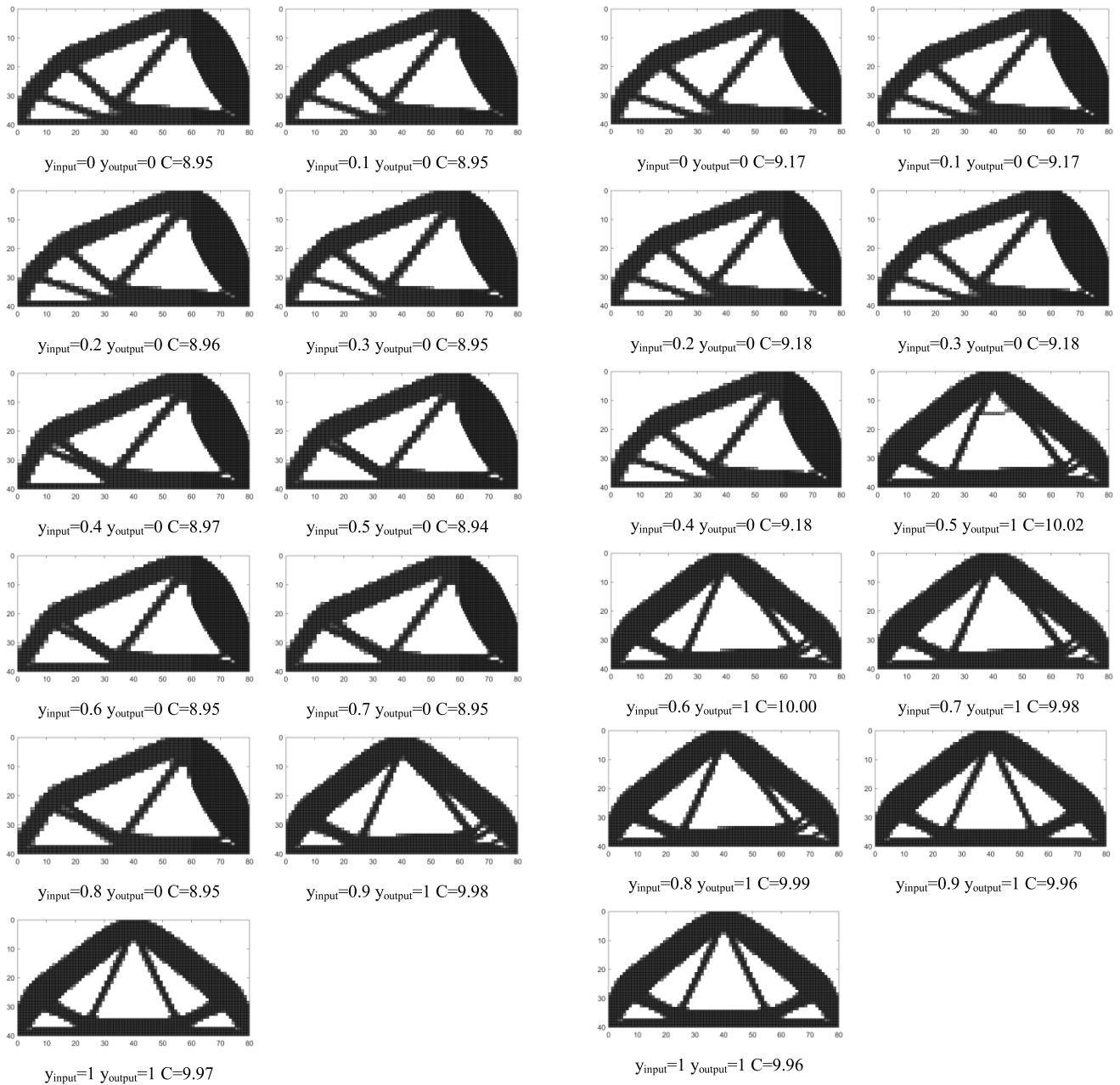


FIGURE 3. Results of the MBB-beam optimization with $q = 1.2$.

the magnitudes of these two sensitivity terms can be in different orders. To ensure the stable and smooth convergence, we update the element densities with the OC method. Given the design variable y , the sensitivity of the volume fraction constraint in (12) is eliminated, while only the sensitivity of the objective function in (11) is considered. Then, the steepest descent method is adopted to update y . In summary, update of the design variable y only picks up the appropriate problem setup, while update of the element densities determines the optimal structural shape and addresses the volume fraction constraint. The numerical examples in Section 3 demonstrate the excellent effect of this novel update strategy.

FIGURE 4. Results of the MBB-beam optimization with $q = 3$.

III. NUMERICAL EXAMPLES

In this section, four numerical examples will be studied to demonstrate the effectiveness of the proposed method. Among them, case 1 adopts the benchmark MBB-beam problem to show the compliance minimization design with different loading conditions; case 2 employs the cantilever problem to show the compliance minimization design with both design domain sizes and loading conditions being different; case 3 focuses on compliant mechanism design with different loading conditions which belongs to a different category of topology optimization problems; a 3D compliance minimization case is studied at the end to show the applicability to 3D problems.

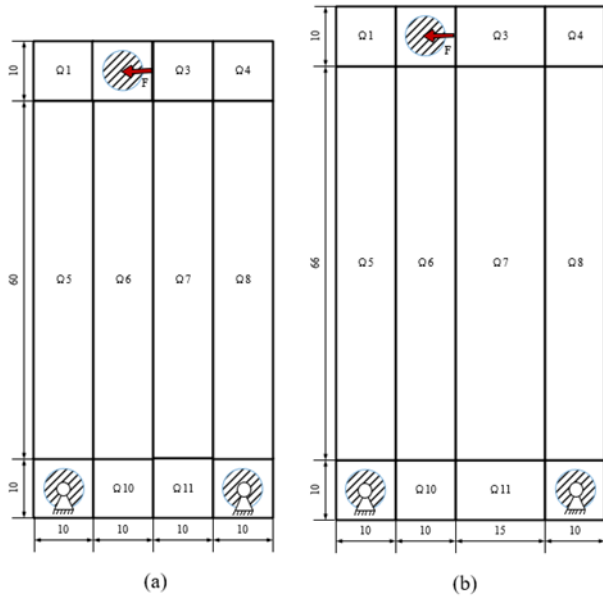


FIGURE 5. Setups of the cantilever problem: (a) the first problem setup; (b) the second problem setup.

A. CASE 1

In the first case, the MBB-beam problem is studied. There are two selective problem setups, as shown in Figure 2, where the design domain sizes are the same of 80*40 but the loading positions are different. The force has the magnitude of 1. The solid material has the Young’s modulus of 1.3 and the Poisson’s ratios of 0.3. The volume fraction limit of this case is 0.5.

As illustrated in Figure 2, the design domain is divided into sub-domains Ω_1 and Ω_2 . Both Ω_1 and Ω_2 of the first problem setup is discretized with finite elements of size 1*1. Ω_1 of the second problem setup is discretized with finite elements of size 1.5*1, and Ω_2 of the second problem setup is filled with elements of size 0.5*1. In this way, the mesh scales are the same of the two problem setups, and the indexes of the loading nodes are identical as well. Therefore, the element stiffness matrix can be formulated with (13).

$$\mathbf{k}(\rho, y) = \rho_e [y^q \bar{\mathbf{k}}_{1 \times 1} + a(1 - y)^q \bar{\mathbf{k}}_{0.5 \times 1} + (1 - a)(1 - y)^q \bar{\mathbf{k}}_{1.5 \times 1}] \tag{13}$$

where $\bar{\mathbf{k}}_{1 \times 1}$, $\bar{\mathbf{k}}_{0.5 \times 1}$, and $\bar{\mathbf{k}}_{1.5 \times 1}$ are the stiffness matrixes of elements with sizes 1*1, 0.5*1, and 1.5*1, respectively. The parameter a (either 0 or 1) is the factor to distinguish between Ω_1 and Ω_2 .

As usual, the penalty p is 3. It should be aware that the optimization problem is initial guess dependent and the initial value of y is crucial for the result. On the other hand, as a robust numerical method, the sensitivity on y should be reduced to the minimum level. Then, the value of q here plays a critical role. The optimization results with $q = 1.2$ and $q = 3$ are demonstrated in Figure 3 and Figure 4, respectively. Different initial guesses of y are explored, varying from 0 to 1 with the interval of 0.1. $y_{output} = 0$ corresponds to

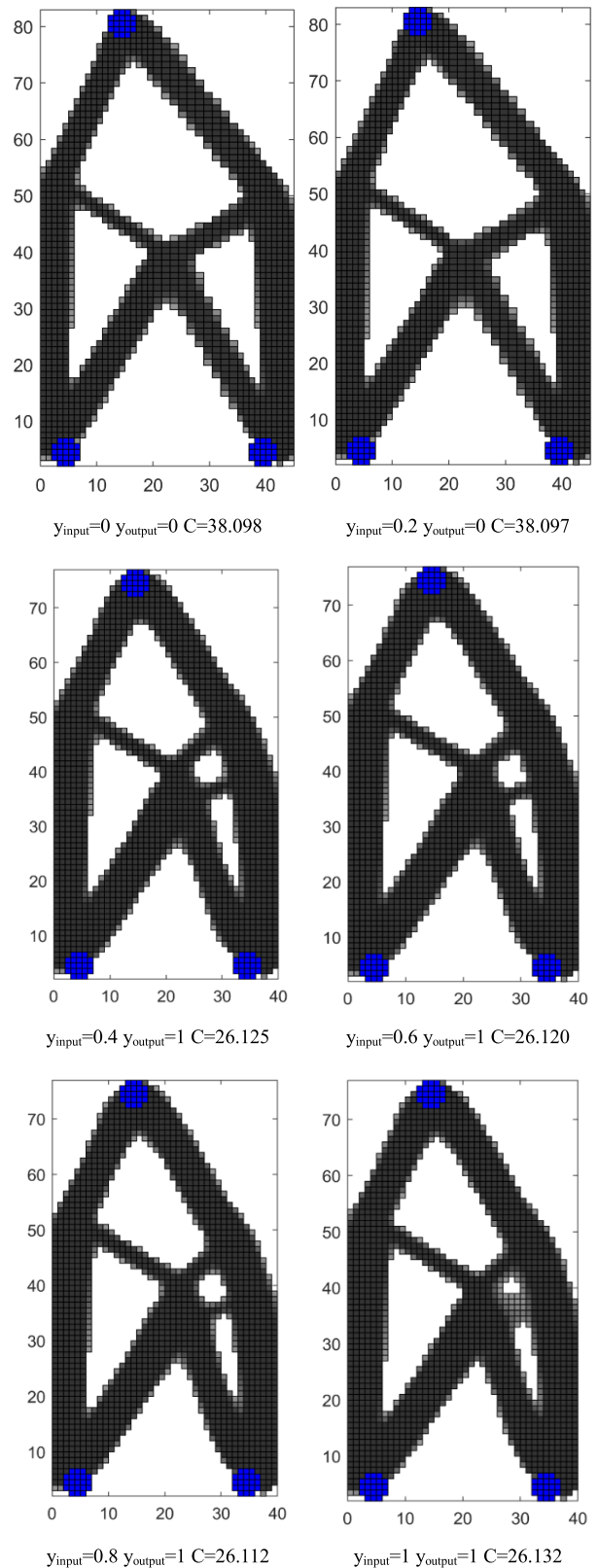


FIGURE 6. Results of the cantilever optimization with $q = 1.2$.

the second problem setup, and $y_{output} = 1$ represents the first problem setup.

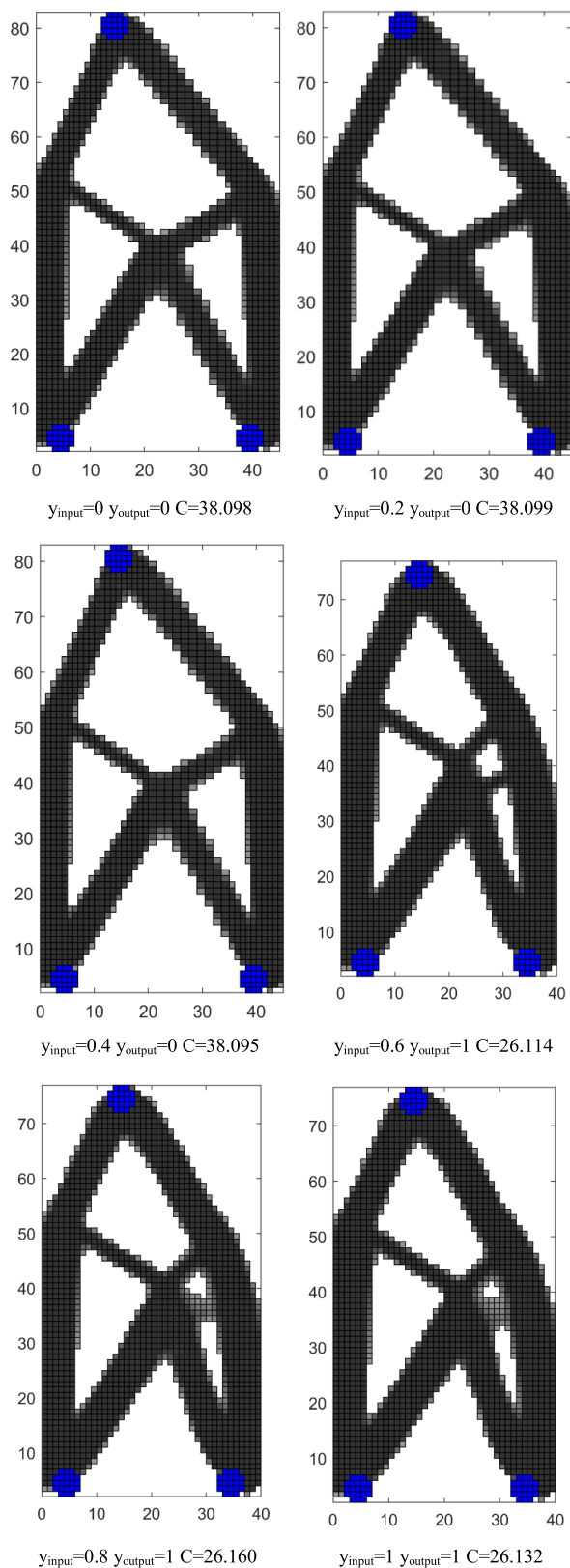


FIGURE 7. Results of the cantilever optimization with $q = 3$.

We can conclude from the results that, optimization with $q = 1.2$ largely eliminates the initial guess dependency issue

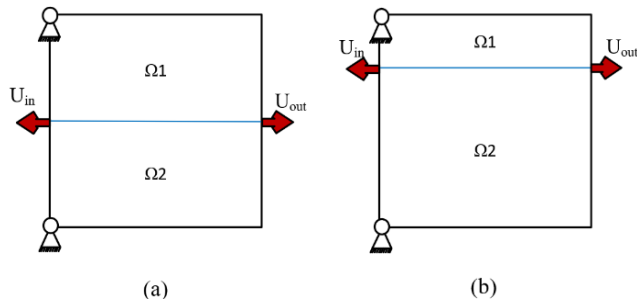


FIGURE 8. Setups of the compliant mechanism problem: (a) sub-domain Ω_1 and Ω_2 both have the size of 60×30 ; (b) sub-domain Ω_1 has the size of 60×15 , and Ω_2 has the size of 60×45 .

since there always makes the selection of the second problem setup ($y_{output} = 0$) with initial guess of $y_{input} = 0 \sim 0.8$. Comparatively, the results with $q = 3$ show strong dependency on the initial guess of y ; in other words, $y_{input} > 0.5$ leads to the $y_{output} = 1$, and $y_{input} < 0.5$ leads to the $y_{output} = 0$. To explain this observation, $q = 3$ makes a strong penalization of the interpolated element stiffness, so that the strain energy densities will be dominated by the first problem setup if $y_{input} > 0.5$, or dominated by the second problem setup if $y_{input} < 0.5$. Instead, the penalization is much weaker with $q = 1.2$, while it still functions well in eliminating intermediate y values in the optimization results.

B. CASE 2

Similar to the first case, there have two selective problem setups of this cantilever problem. The design domain sizes are shown in Figure 5 where the shaded circular areas are non-designable. The force has the magnitude of 1. The solid material has the Young's modulus of 1.3 and the Poisson's ratios of 0.3. The volume fraction limit of this case is 0.5.

To realize an integrated problem formulation, the design domains are divided into 12 sub-domains: $\Omega_1 \sim \Omega_{12}$. The $\Omega_1 \sim \Omega_{12}$ of the first problem setup are discretized with uniform finite elements of 1×1 , while the $\Omega_1 \sim \Omega_{12}$ of the second problem setup are discretized with heterogeneous finite elements of sizes: $1 \times 1, 1 \times 1, 1.5 \times 1, 1 \times 1, 1 \times 1.1, 1 \times 1.1, 1.5 \times 1.1, 1 \times 1.1, 1 \times 1, 1 \times 1, 1.5 \times 1, 1 \times 1$, respectively. Again, the purpose of this heterogeneous meshing is to ensure the same mesh scale between the two problem setups, and to guarantee the indexes of the loading and fixing nodes are identical.

To further explore the effect of q value. The optimization results with $q = 1.2$ and $q = 3$ are demonstrated in Figure 6 and Figure 7, respectively. Different initial guesses of y are explored, varying from 0 to 1 with the interval of 0.2. $y_{output} = 0$ corresponds to the second problem setup, and $y_{output} = 1$ represents the first problem setup. From the numerical results, the same conclusion can be drawn as compared with case 1.

C. CASE 3

In this case, we extended the algorithm to solve the compliant mechanism design problem: to maximize the inverse

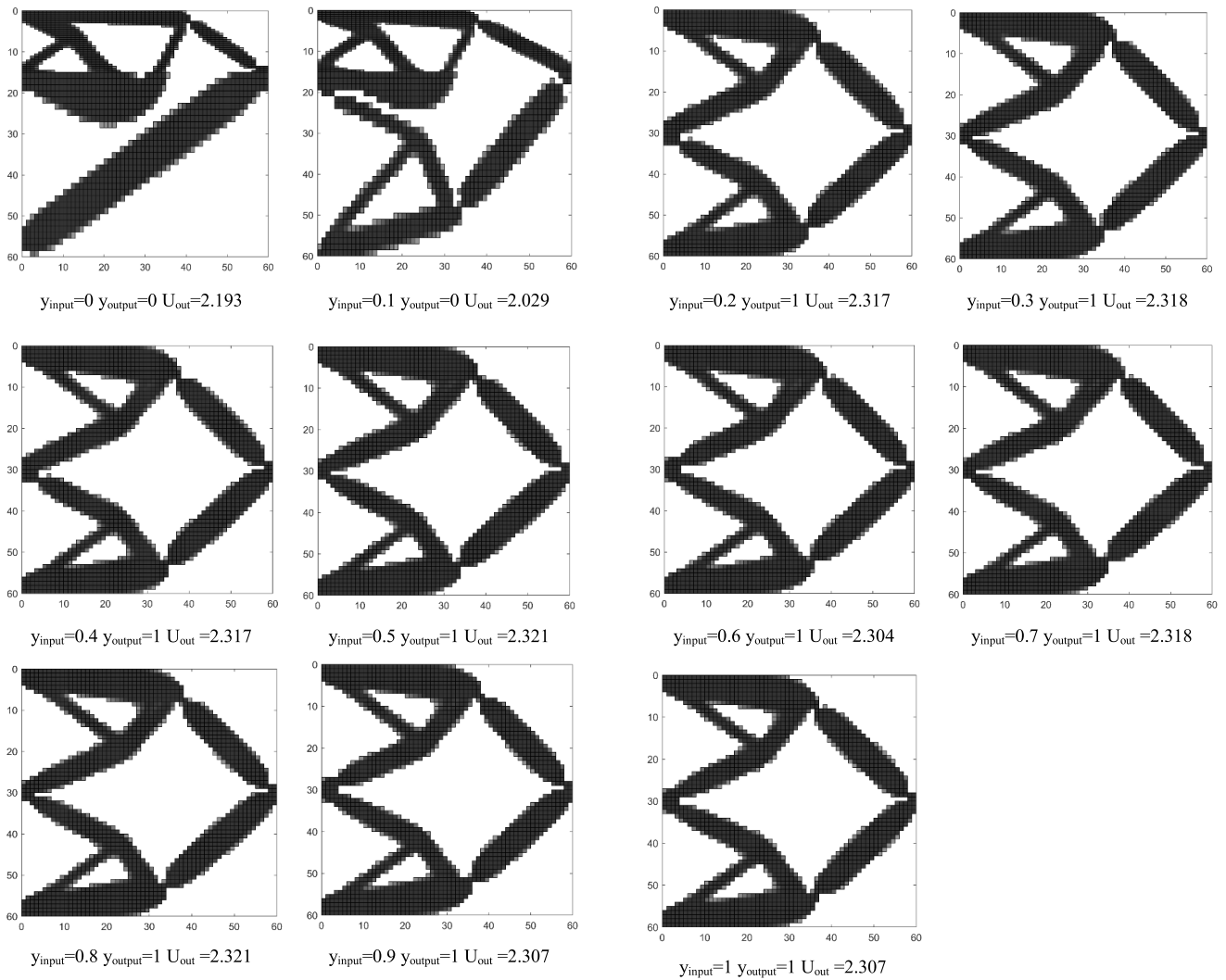


FIGURE 9. Results of the compliant mechanism optimization with $q = 1.2$.

displacement output with a displacement input. There are still two selective problem setups, as shown in Figure 8, where the design domain sizes are the same of 80×40 but the boundary conditions are different. The displacement input has the magnitude of 1. The material properties are used as the last two examples. The volume fraction limit of this case is 0.4. With this case, the Method of Moving Asymptotes (MMA) [45] is adopted as the optimizer.

As illustrated in Figure 8, the design domain is divided into sub-domains Ω_1 and Ω_2 . Both Ω_1 and Ω_2 of the first problem setup is discretized with finite elements of size 1×1 . Ω_1 of the second problem setup is discretized with finite elements of size 1×0.5 , and Ω_2 of the second problem setup is filled with elements of size 1×1.5 . In this way, the mesh scales are the same of the two problem setups, and the indexes of the input and output nodes are identical as well.

With this case, only the optimization results with $q = 1.2$ are demonstrated in Figure 9. Different initial guesses of y are explored, varying from 0 to 1 with the interval of 0.1.

$y_{output} = 0$ corresponds to the second problem setup, and $y_{output} = 1$ represents the first problem setup. We can see that, even though a different type of optimization problem was studied, there still can research the consistent conclusion: the optimization largely eliminates the initial guess dependency issue since there always makes the selection of the first problem setup ($y_{output} = 1$) with initial guess of $y_{input} = 0.2 \sim 1$. The derived displacement output of the first problem setup is evidently better than that of the second problem setup.

D. CASE 4

In the last case, a 3D design for additive manufacturing case will be investigated. Two additive manufacturing devices (Fused Filament Fabrication, FFF) with chambers of different sizes. As shown in Figure 10, chamber size of the first machine is $36 \times 25 \times 20$ and that of the second machine is $30 \times 30 \times 20$. Then, a bridge-like structure will be designed that will be manufacture with one of the machines. The boundary condition is show in Figure 10 (c), and the design

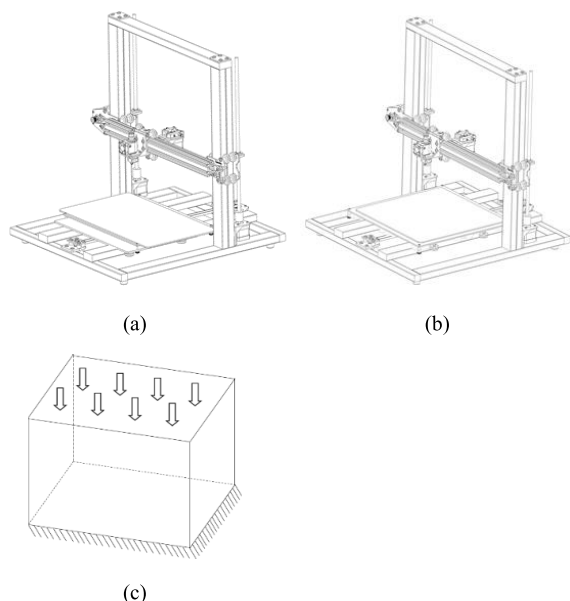


FIGURE 10. Problem setups of the design for additive manufacturing case. (a) The first FFF machine with chamber size of 36*25*20 that prints Peek (Young’s modulus is 3.8 GPa, and the Poisson’s ratio is 0.172); (b) the second FFF machine with chamber size of 30*30*20 that prints ABS (Young’s modulus is 2.0 GPa, and the Poisson’s ratio is 0.394); (c) boundary condition of the bridge-like structural optimization problem.

domains of the two problem setups will just be the chambers. Moreover, the machines use two kinds of materials: Peek for the first machine and ABS for the second. A compliance minimization problem will be solved to concurrently design the structural shape and select the appropriate machine. The material volume fraction limit is 0.3. The top two layers of elements will be inactive (always solid) during optimization.

The optimization results with $q = 1.2$ are demonstrated in Figure 11. Different initial guesses of y are explored, varying from 0 to 1 with the interval of 0.1. $y_{output} = 0$ corresponds to the first problem setup, and $y_{output} = 1$ represents the second problem setup. A consistent conclusion can be drawn from this case that the optimization at most times could pick up the better problem setup with initial guesses of $y_{input} = 0 \sim 0.9$. Therefore, this again proves the effectiveness of the proposed topology optimization method with selective problem setups to concurrently select the appropriate problem setup and derive the optimized structural shape.

At the end, the computing time is briefly discussed. This 3D case was run on a desktop computer with Intel Xeon W-2145 CPU and 64GB RAM. Matlab R2018b was used to run the program. Then, the 11 cases of Figure 11 took 648s in average. The computing time of problem setup (a) with the traditional SIMP method took 641s, and the computing time of problem setup (b) took 612s to converge. Therefore, we can conclude that nearly half of the time was saved with the new method to concurrently pick up the better problem setup and derive the optimal structural topology.



FIGURE 11. Results of bridge-like structure design.

IV. CONCLUSION

In this paper, the novel topology optimization method has been developed to address the design efficiency issue when multiple problem setups are involved. A novel meshing strategy and material interpolation model are proposed to unify the multiple problem setups into a single optimization problem. Therefore, the optimization algorithm only runs once to concurrently derive the optimal structural shape and the

best problem setup choice in a very efficient manner. Ideally, only $1/N$ of the computational cost is needed compared to the traditional topology optimization methods that solve the different problem setups separately. Here, N means the number of candidate problem setups. Several numerical examples are studied that have proved the effectiveness of the proposed method.

On the other hand, this is still the first work that only addresses compliance-minimization problems and compliant mechanism problems. To make it general, the method should be extended to robustly address more complex physics such as the natural frequency design and the stress-related problems. Therefore, the extension will be the focus of our future work.

ACKNOWLEDGMENT

(Junyu Fu and Jiaqi Huang contributed equally to this work). The authors would like to thank the support from the Qilu Young Scholar Award, Shandong University.

REFERENCES

- [1] M. P. Bendsøe and N. Kikuchi, "Generating optimal topologies in structural design using a homogenization method," *Comput. Method Appl. Mech. Eng.*, vol. 71, no. 2, pp. 197–224, 1988.
- [2] M. P. Bendsøe and O. Sigmund, *Topology Optimization: Theory, Methods, and Applications*. Berlin, Germany: Springer, 2003.
- [3] M. Y. Wang, X. Wang, and D. Guo, "A level set method for structural topology optimization," *Comput. Methods Appl. Mech. Eng.*, vol. 192, nos. 1–2, pp. 227–246, Jan. 2003.
- [4] G. Allaire, F. Jouve, and A.-M. Toader, "A level-set method for shape optimization," *Comput. Rendus Math.*, vol. 334, no. 12, pp. 1125–1130, Jan. 2002.
- [5] Y. M. Xie and G. P. Steven, *Evolutionary Structural Optimization*. London, U.K.: Springer, 1997.
- [6] X. Guo, W. Zhang, and W. Zhong, "Doing topology optimization explicitly and geometrically—a new moving morphable components based framework," *J. Appl. Mech.*, vol. 81, no. 8, 2014, Art. no. 081009.
- [7] G. I. N. Rozvany, "A critical review of established methods of structural topology optimization," *Struct. Multidisciplinary Optim.*, vol. 37, no. 3, pp. 217–237, 2009.
- [8] O. Sigmund and K. Maute, "Topology optimization approaches," *Struct. Multidisciplinary Optim.*, vol. 48, no. 6, pp. 1031–1055, Dec. 2013.
- [9] N. P. van Dijk, K. Maute, M. Langelaar, and F. van Keulen, "Level-set methods for structural topology optimization: A review," *Struct. Multidisciplinary Optim.*, vol. 48, no. 3, pp. 437–472, Sep. 2013.
- [10] J. Liu and Y. Ma, "A survey of manufacturing oriented topology optimization methods," *Adv. Eng. Softw.*, vol. 100, pp. 161–175, 2016.
- [11] D. Shi, H. Ma, and X. Teng, "A structure topology optimization with the first-order saddlepoint approximation," *IEEE Access*, vol. 7, pp. 98174–98181, 2019.
- [12] L. Yin, F. Zhang, X. Deng, P. Wu, H. Zeng, and M. Liu, "Isogeometric bi-directional evolutionary structural optimization," *IEEE Access*, vol. 7, pp. 91134–91145, 2019.
- [13] H.-Y. Jiao, Y. Li, and L.-Y. Yang, "Periodic layout optimization of cyclic symmetric structure," *IEEE Access*, vol. 7, pp. 55269–55276, 2019.
- [14] M. Pedroza-Villalba, E. A. Portilla-Flores, E. Vega-Alvarado, M. B. Calva-Yáñez, E. Santiago-Valentín, and E. Alcalá-Fazio, "Truss topology optimization based on a birth/death element approach," *IEEE Access*, vol. 6, pp. 72609–72619, 2018.
- [15] O. Sigmund, "Manufacturing tolerant topology optimization," *Acta Mech. Sin.*, vol. 25, no. 2, pp. 227–239, Mar. 2009.
- [16] F. Wang, B. S. Lazarov, and O. Sigmund, "On projection methods, convergence and robust formulations in topology optimization," *Struct. Multidisciplinary Optim.*, vol. 43, no. 6, pp. 767–784, 2011.
- [17] M. Schevenels, B. S. Lazarov, and O. Sigmund, "Robust topology optimization accounting for spatially varying manufacturing errors," *Comput. Methods Appl. Mech. Eng.*, vol. 200, nos. 49–52, pp. 3613–3627, Dec. 2011.
- [18] S. Chen and W. Chen, "A new level-set based approach to shape and topology optimization under geometric uncertainty," *Struct. Multidisciplinary Optim.*, vol. 44, no. 1, pp. 1–18, Jul. 2011.
- [19] W. Zhang and Z. Kang, "Robust shape and topology optimization considering geometric uncertainties with stochastic level set perturbation," *Int. J. Numer. Methods Eng.*, vol. 110, no. 1, pp. 31–56, Apr. 2017.
- [20] J. Liu and Y. Ma, "Sustainable design-oriented level set topology optimization," *J. Mech. Des.*, vol. 139, no. 1, pp. 011403-1–011403-8, 2017.
- [21] G. Prevati, F. Ballo, and M. Gobbi, "Concurrent topological optimization of two bodies sharing design space: Problem formulation and numerical solution," *Struct. Multidisciplinary Optim.*, vol. 59, no. 3, pp. 745–757, Mar. 2019.
- [22] J. Liu and Y.-S. Ma, "3D level-set topology optimization: A machining feature-based approach," *Struct. Multidisciplinary Optim.*, vol. 52, no. 3, pp. 563–582, 2015.
- [23] J. Liu, Y. Zheng, Y. Ma, A. Qureshi, and R. Ahmad, "A topology optimization method for hybrid subtractive-additive remanufacturing," *Int. J. Precis. Eng. Manuf.-Green Technol.*, pp. 1–15, 2019.
- [24] J. Liu, "Current and future trends in topology optimization for additive manufacturing," *Struct. Multidisciplinary Optim.*, vol. 57, pp. 2457–2483, 2018.
- [25] P. Zhang, "Efficient design-optimization of variable-density hexagonal cellular structure by additive manufacturing: Theory and validation," *J. Manuf. Sci. Eng.*, vol. 137, no. 2, 2015, Art. no. 021004.
- [26] Y. Wang, S. Arabnejad, M. Tanzer, and D. Pasini, "Hip implant design with three-dimensional porous architecture of optimized graded density," *J. Mech. Des.*, vol. 140, no. 11, 2018, Art. no. 111406.
- [27] A. du Plessis, I. Yadroitsava, I. Yadroitssev, S. le Roux, and D. C. Blaine, "Numerical comparison of lattice unit cell designs for medical implants by additive manufacturing," *Virtual Phys. Prototyp.*, vol. 13, no. 4, pp. 266–281, 2018.
- [28] D. Shamvedi, O. J. McCarthy, E. O'Donoghue, C. Danilenkoff, P. O'Leary, and R. Raghavendra, "3D Metal printed heat sinks with longitudinally varying lattice structure sizes using direct metal laser sintering," *Virtual Phys. Prototyp.*, vol. 13, no. 4, pp. 301–310, 2018.
- [29] Y. Wang, F. Chen, and M. Y. Wang, "Concurrent design with connectable graded microstructures," *Comput. Methods Appl. Mech. Eng.*, vol. 317, pp. 84–101, Apr. 2017.
- [30] H. Li, Z. Luo, L. Gao, and Q. Qin, "Topology optimization for concurrent design of structures with multi-patch microstructures by level sets," *Comput. Methods Appl. Mech. Eng.*, vol. 331, pp. 536–561, Apr. 2018.
- [31] J. Liu, Y. Zheng, R. Ahmad, J. Tang, and Y. Ma, "Minimum length scale constraints in multi-scale topology optimisation for additive manufacturing," *Virtual Phys. Prototyp.*, vol. 14, no. 3, pp. 229–241, 2019.
- [32] H. Yu, J. Huang, B. Zou, W. Shao, and J. Liu, "Stress-constrained shell-lattice infill structural optimization for additive manufacturing," *Virtual Phys. Prototyp.*, pp. 1–14, 2019.
- [33] H. Zhang, Y. Wang, and Z. Kang, "Topology optimization for concurrent design of layer-wise graded lattice materials and structures," *Int. J. Eng. Sci.*, vol. 138, pp. 26–49, 2019.
- [34] A. Clausen, N. Aage, and O. Sigmund, "Exploiting additive manufacturing infill in topology optimization for improved buckling load," *Engineering*, vol. 2, no. 2, pp. 250–257, 2016.
- [35] J. Wu, N. Aage, R. Westermann, and O. Sigmund, "Infill optimization for additive manufacturing—Approaching bone-like porous structures," *IEEE Trans. Vis. Comput. Graph.*, vol. 24, no. 2, pp. 1127–1140, Feb. 2018.
- [36] A. T. Gaynor, N. A. Meisel, C. B. Williams, and J. K. Guest, "Multiple-material topology optimization of compliant mechanisms created via poly-jet three-dimensional printing," *J. Manuf. Sci. Eng.*, vol. 136, no. 6, Oct. 2014, Art. no. 061015.
- [37] J. Liu and Y. Ma, "A new multi-material level set topology optimization method with the length scale control capability," *Comput. Methods Appl. Mech. Eng.*, vol. 329, pp. 444–463, Feb. 2018.
- [38] S. K. Chandrasegaran, "The evolution, challenges, and future of knowledge representation in product design systems," *Comput.-Aided Des.*, vol. 45, no. 2, pp. 204–228, Feb. 2013.
- [39] P. Zhang, J. Liu, and A. C. To, "Role of anisotropic properties on topology optimization of additive manufactured load bearing structures," *Scr. Mater.*, vol. 135, pp. 148–152, Jul. 2017.

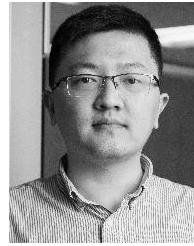
- [40] M. P. Bendsøe, "Optimal shape design as a material distribution problem," *Struct. Optim.*, vol. 1, no. 4, pp. 193–202, Dec. 1989.
- [41] G. I. N. Rozvany, M. Zhou, and T. Birker, "Generalized shape optimization without homogenization," *Struct. Optim.*, vol. 4, no. 3, pp. 250–252, Sep. 1992.
- [42] A. Díaz and O. Sigmund, "Checkerboard patterns in layout optimization," *Struct. Optim.*, vol. 10, no. 1, pp. 40–45, Aug. 1995.
- [43] O. Sigmund and J. Petersson, "Numerical instabilities in topology optimization: A survey on procedures dealing with checkerboards, mesh-dependencies and local minima," *Struct. Optim.*, vol. 16, no. 1, pp. 68–75, Aug. 1998.
- [44] O. Sigmund, "A 99 line topology optimization code written in MATLAB," *Struct. Multidisciplinary Optim.*, vol. 21, no. 2, pp. 120–127, Apr. 2001.
- [45] K. Svanberg, "MMA and GCMMA—two methods for nonlinear optimization," *Tech. Rep.*, 2007.



JUNYU FU received the Ph.D. degree in mechanical engineering from the University of Alberta, Canada, in 2018. He is currently an Assistant Professor with the College of Mechanical and Vehicle Engineering, Taiyuan University of Technology, China. His research interests include plastic injection molding, design optimization, and CAD/CAE/CAM.



JIAQI HUANG received the bachelor's degree from Jilin University, Changchun, China, in 2013. He is currently pursuing the Ph.D. degree with Shandong University. His research interests include topology optimization, additive manufacturing, and soft robotics.



JIKAI LIU received the Ph.D. degree from the University of Alberta, Canada. He was a Postdoctoral Research Associate with the ANSYS Additive Manufacturing Research Laboratory, University of Pittsburgh, USA. He is currently a Professor with the School of Mechanical Engineering, Shandong University, China. His main research is focused on topology optimization, additive manufacturing, and engineering informatics.

...